Janusz HETMAŃCZYK, Tomasz STENZEL, Bogusław GRZESIK

Silesian University of Technology, Faculty of Electrical Engineering,
Department of Power Electronics, Electrical Drives and Robotics

Selected aspects of design and modelling of linear actuator based on PM BLDC motor

Abstract. The article describes process of design and modeling PM BLDC motor operating in a linear actuator. The actuator drive mechanism is implemented on base of a ball screw. The possibility of applying the simplifications consequent by the need for the implementation of model real-time calculation was considered. The differences in the results generated using such models in comparison to the full model was also taken into account. Furthermore, it was presented the structure of the real actuator control system. The results of computer simulations were compared with the measurements waveforms, obtained on the test bench. **(Wybrane aspekty projektowania i modelowania siłownika liniowego zrealizowanego na bazie silnika PM BLDC)**

Streszczenie. W artykule opisano proces projektowania i modelowania silnika PM BLDC pracującego w siłowniku liniowym. Mechanizm posuwu siłownika realizowany jest na śrubie kulowej. Rozważono możliwości stosowania uproszczeń wynikających z potrzeby realizacji obliczeń w czasie rzeczywistym. W badaniach uwzględniono różnice w wynikach generowanych przy użyciu modeli uproszczonych w porównaniu do modeli pełnych. Ponadto zaprezentowano strukturę układu sterowania rzeczywistym siłownikiem. Uzyskane wyniki symulacji komputerowych zestawiono z przebiegami pomiarowymi otrzymanymi na stanowisku badawczym.

Keywords: Permanent magnet brushless, electric drive, linear actuator, modeling
Słowa kluczowe: Bezszczotkowy silnik prądu stałego, napęd elektryczny, siłownik liniowy, projektowanie i modelowanie

Introduction

The subject of the paper is the numeric model of a linear actuator designed for a six motor drive of a parallel manipulator. Control of the above mentioned manipulator requires at first the development of the six motor drive control structure. Another requirement is an implementation of inverse kinematics or even, in particular cases, inverse dynamics solution. When kinematic description of the manipulator is sufficient, the results of algebraic or numeric calculation are setpoints of actuators stroke controller. Considering the accelerations of six actuators, it might be necessary to calculate inverse dynamics solution of parallel manipulator and limit each actuator currents in order to achieve appropriate accelerations. Thus the model of single actuator is a fundamental component of the parallel manipulator complex numeric model. The development and laboratory verification of such a model is described in the paper.

The ancestor of systems with parallel structure is a movable platform based on six telescopic actuators, which are joined with ball joints. That device was designed by Gough in 1947. But in 1965 the design known as Stewart platform was contributed to the theory of machines. In that time Stewart developed parallel structure with six degrees of freedom for a flight simulator. There exists also a term Stewart-Gough platform [17, 16]. Mechanical system of this design are used for the construction of aircraft flight or driving vehicle simulators. Another branch of applications of the abovementioned systems is a design of test stands for analysis of impacts of the vibrations and shocks on the tested system operation. Parallel manipulators like Stewart-Gough design are also used as stabilization system in medical conveyances for patient protection in cases of spinal injuries or in neonatal transport as well as in special transport area for sensitive goods protection.

There are some advantages of parallel manipulators, starting from the possibility of six degrees of freedom motion, through the possibility of high accelerations and velocities due to small masses of moving parts and finishing with high positioning accuracy resulting from the high rigidity of the mechanism. Besides Stewart-Gough parallel manipulator is characterized by advantageous weight to volume ratio. It is also worth to mention that all the drives of that system are identical, which leads to better efficiency and higher loads of the manipulator.

There are also few disadvantages of parallel manipulators like limitations of working space, which is often much smaller than the dimensions of the platform. The other drawbacks are: possibility of conflict between the kinematic chain elements, presence of singular points within the workspace, the difficulty in determining direct geometric-kinematic parameters, complex control system, the complexity of the linkages between the moving kinematic chains.

Figures 1a and 1b show the types of kinematic chains of linear actuator used in parallel manipulators. Both kinematic chains have three types of joints in different configuration: universal U, prismatic P, and spherical S. Design principles of prismatic joints P based on ball screw are described in detail by [1] and [10].

Beside the classical kinematics platform 6-UPS (Figure 2a) proposed by Gough-Stewart and then [2] or [18] and [5] based on linear actuators, it is known and used in modified solutions. Such kinematics is shown in Figure 2b. It developed the novel platform 6-PSU, which consists of six legs with a prismatic joint P, spherical joint S, and universal joint U [4]. The six prismatic joints move vertically with respect to the base, which appears to be a significant improvement over the standard Gough-Stewart platform. The same 6-PSU kinematic diagram of the parallel manipulator was proposed by [15]. In the analyzed cases, each linear actuator consists of a drive and joints: the universal U, prismatic P, and spherical S. Usually, the authors do not focus on the modeling of DC drive but the acceleration-based force-impedance controller. In one case, classic mini DC motors (15W, 18 V and 5300 rpm) were used [15]. The authors present a dynamic model of the DC drive as an element of the Robotic Controlled Impedance Device (RCID). In another case, the model of 6-UPS platform was developed based on permanent magnet synchronous motors [18]. This type of kinematics is shown in Figure 2a.
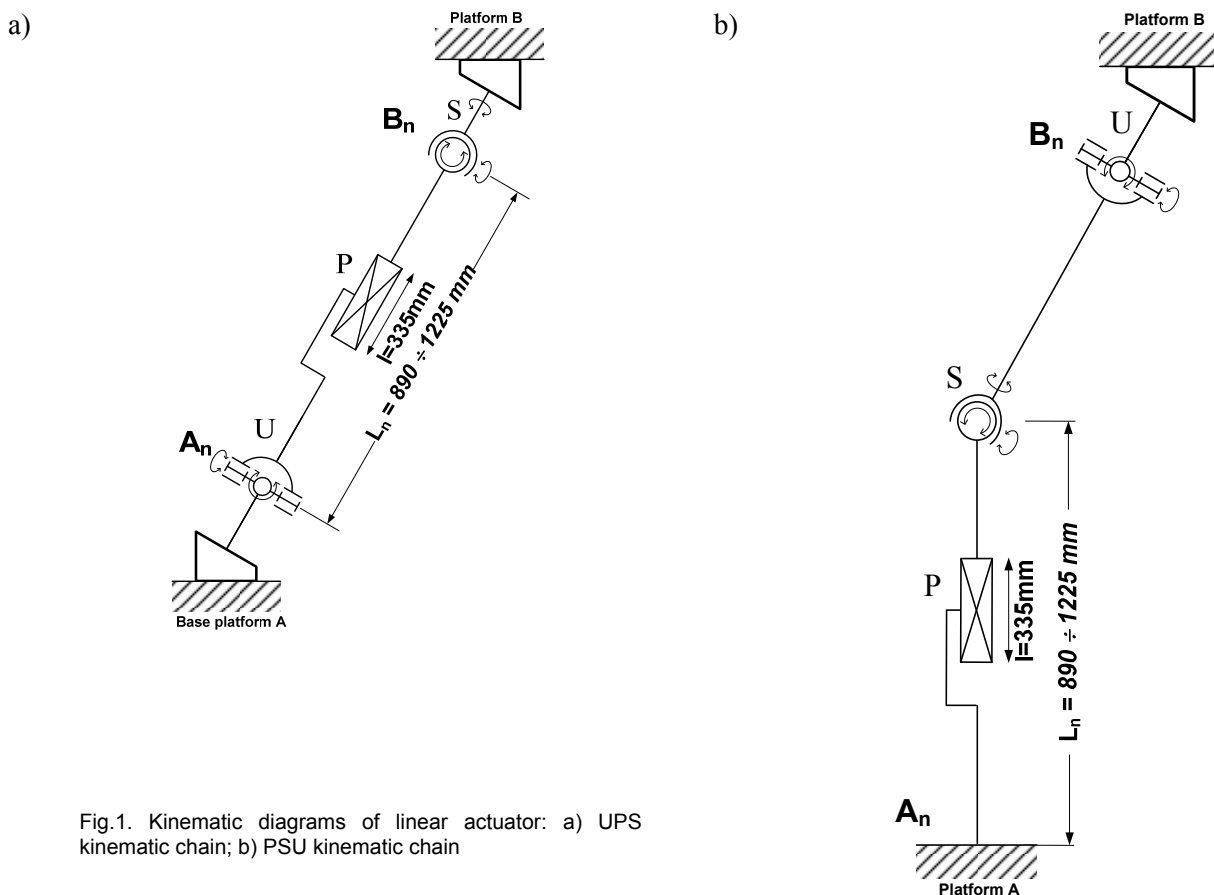
.

a)

b)

Fig.1. Kinematic diagrams of linear actuator: a) UPS kinematic chain; b) PSU kinematic chain

The same kinematics of 6-UPS platform driven by hydraulic linear actuators were used as a motion simulator [6]. The paper proposes three systematic optimal design procedures to solve the practical design problems of the Gough-Stewart platform and the authors focus on the modeling of electrohydraulic linear actuator. There is one article dedicated to modeling of PM BLDC linear actuator drive [20], but in the paper [9] describe model of PM BLDC designed to gear servo actuator. Quite similar 6-3 UPS kinematics of parallel manipulator is presented in [8]. It is illustrated in Figure 2c. The 6-3 UPS parallel manipulator consists of six linear actuators connected to the base platform in six points via universal joints U, and to the motion platform in three points via spherical joints S. Consequently, the consecutive linear actuators are linked to each other in three pairs.

The linear actuator as an application of a parallel manipulator

Parallel manipulator operating in six degrees of freedom (6DOF) consists of a fixed lower base and movable upper platform. These parts are connected with six independent linear actuators (Figure 3a). Each of the actuators, also called arms of the manipulator, is made up of two main parts connected with a screw driven by motor and a ball nut. Those parts of the whole mechanism enable conversion of rotary to progressive motion. The screw is propelled by permanent magnet brushless DC motor (PM BLDC). Lower part of the arm is connected with the base with the Cardan joint, while upper part of the arm is linked to the upper platform with mechanical system, which includes Cardan joint and rotary universal joint. Control of the described parallel manipulator is based on an appropriate setting of each actuator length, which leads to achieving six degree of freedom for the upper platform of the manipulator. PM BLDC motors of 400 W were used in

the drive system of each actuator. The motors were equipped with integrated control unit controlling the velocity, current, and position of the motor. The motion parameters including the rotation direction and the number of pulses of the encoder can be set using the CANopen protocol.

Control methods of parallel manipulators

Control methods of parallel manipulators can be classified in respect of mathematical description form and the accuracy of manipulator positioning derived from that [21, 19]. In this perspective the parallel manipulator control algorithms can be divided into two categories: first-based on the analytical methods, and second - based on numerical calculations. Specific algorithms of parallel manipulator motion control differ mainly in positioning accuracy and computational complexity.

Typical description of the parallel manipulator is based on the three dimensional Cartesian coordinates (X_B, Y_B, Z_B) and three angles (θ, φ, ψ). It is shown in the Figure 3b. The central point of the manipulator is the center of the local coordinate system of the manipulator, while the central point of lower base Q_A is the center of the global base coordinate system. The points from A_1 to A_6 describe the manipulator base. The upper platform of the manipulator is defined by points B_1 to B_6. The mentioned two parts of the manipulator are linked with six linear actuators labeled as L_1, L_2, L_3, L_4, L_5 and L_6. Vector p is the orientation vector of the coordinate Q_B with respect to Q_A. The position vector a_i (related to Q_A), b_i - the position vector (related to Q_B). The idea of the algorithm of the manipulator control lies in determination of the upper platform translations and rotations in three dimensions. Depending of the desired motion parameters, position and orientation or even acceleration in three dimensions are determined.
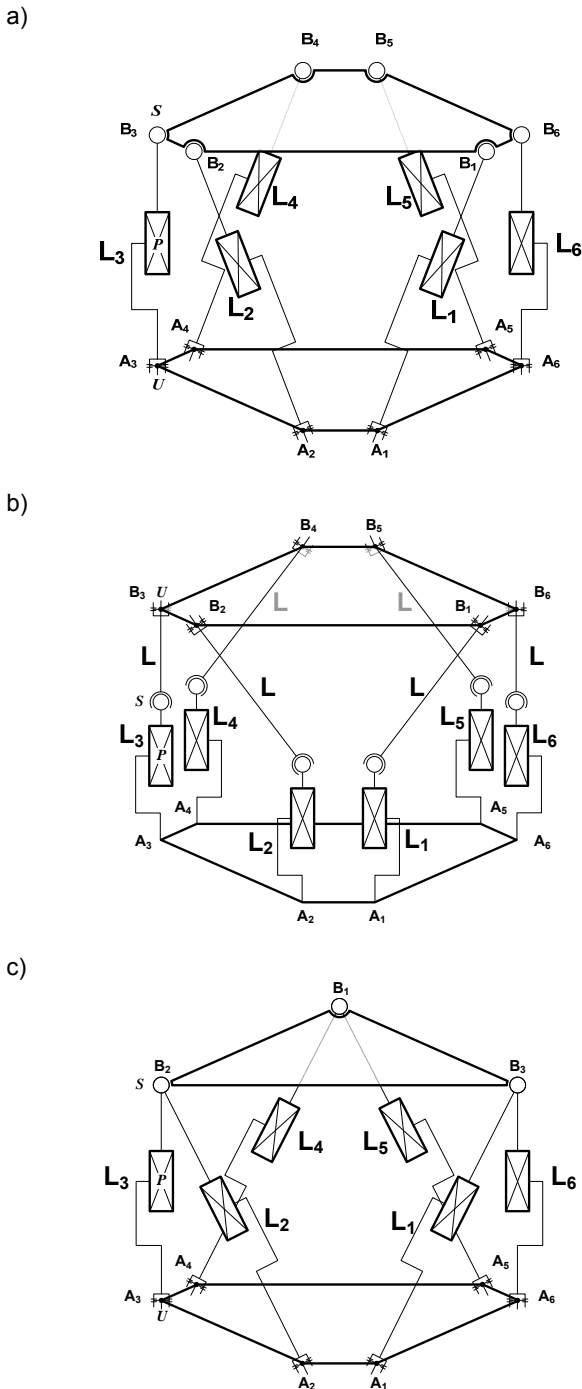
a)

b)

c)

Fig.2. Kinematics diagram of Stewart-Gough parallel manipulator: a) the 6-UPS parallel manipulator; b) the 6-PSU parallel manipulator; c) the 6-3 UPS parallel manipulator.

When, translations, called also actuator strokes are known, the calculation of motion is described as forward kinematics. The inverse kinematics algorithm allows to determine strokes of all actuators in assumption of desired change of positions of manipulator upper platform. This control method requires determination of all angular and linear translation values, which are possible within certain constraints of linkages and which lead to desired position of the upper platform of the parallel manipulator. The solution of inverse kinematics is the main task of control and motion programming for parallel manipulators. This is important when determining manipulator motion in time. The inverse kinematic solution leads to determination

of the values of controls for each linear actuator drive. In such approach the torques, inertias and forces, present when the manipulator is in motion, are omitted. In order to achieve accurate values of actuator controls, corresponding to the values of the real mechanical system, it is necessary to solve inverse dynamics task.
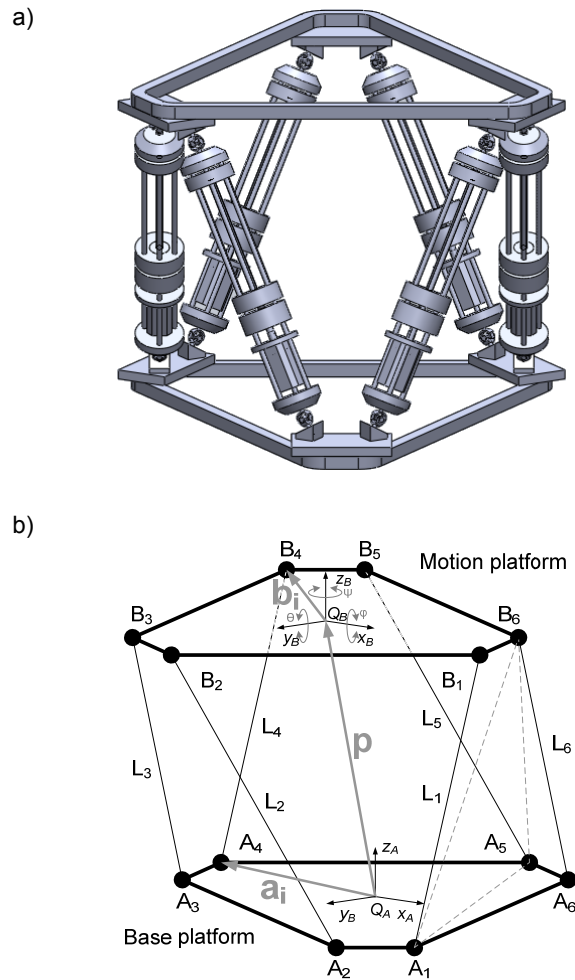
a)

b)

Fig.3. CAD model of 6DOF parallel manipulator: a) design; b) kinematic model

Design of the linear actuator for parallel manipulator

We have used the SolidWorks software package for the development of linear actuator design. This engineering Computer Aided Design (CAD) tool allows not only for three dimensional models design, but as well allows for examination of designed mechanical elements in respect of the selected issues of kinematics, dynamics and endurance. The design process has been started from making the assumptions concerning kinematics and manufacturing materials. Then three-dimensional model has been designed and it has been used for determination of selected endurance parameters. The final shape of the designed actuator is shown in the Figure 5. As the examples of computer analysis made in SolidWorks environment in the Figure 4 we have shown load force and load torque of the designed linear actuator during vertical motion cycle of the parallel manipulator.
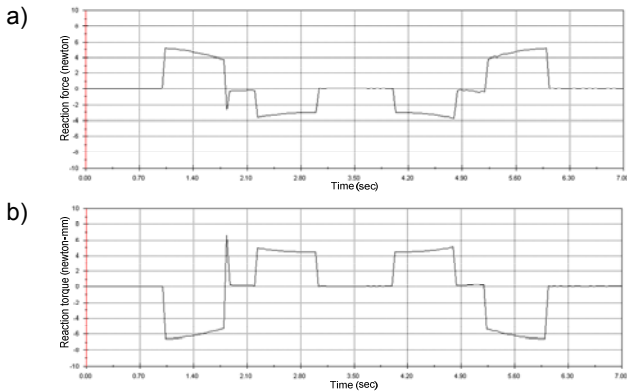
a)

b)

Fig.4. The waveforms of a) ball screw load force of single linear actuator; and b) load torque of this actuator PM BLDC motor drive, during full vertical movement of the parallel manipulator

The linear actuator presented in Figure 5 is based on the cage framework consisting of six hexagonal aluminum discs, connected with six connected circular steel rods. Three of these rods are firmly fixed with both motor body and the ball screw. The pitch of the used ball screw is $p_{scr}= 5$ mm. A shaft of the PM BLDC motor is linked to the ball screw with a clutch. The ball screw is mounted in upper and lower ball bearing. The motor, ball screw and fixing bearing make a complete drive mechanism. Lower bearing block consists of two ball bearings, while upper bearing block is made of single ball bearing. The translation mechanism consists of three remaining leading rods fixed to the ball screw. Possible translation of this mechanism is $l= 335$mm. Fixing and leading rods are led by linear bearings, which are mounted in the holes in the hexagonal discs. The rod endings are fixed in the appropriate discs with axial and radial screw connections [10]. Minimal length of each actuator is $L_{min}= 890$ mm.
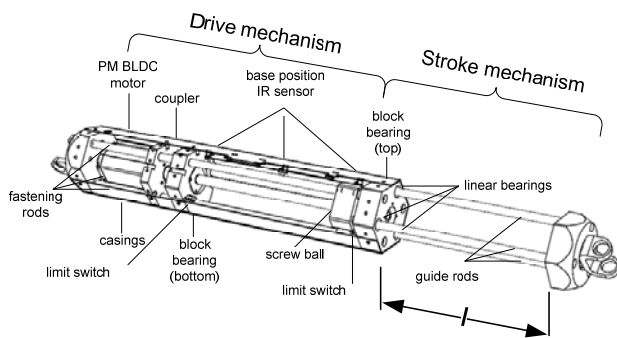

Fig.5. The design of linear actuator with PMBLDC motor

For designing the three-dimensional model of the parallel manipulator (Figure 3a) we have used the linear actuator model, which we designed in SolidWorks CAD environment. We have designed the parallel manipulator model in order to make analysis of that electromechanical device and also in order to make a synthesis of its control system structure and parameters. That approach, based on integration of CAD software with simulation environment was previously described in a few publications for example in [3]. We have used Matlab/ Simulink model compatible with SimMechanics toolbox prepared from the data automatically exported from the previously designed three-dimensional model. The described design process sequence allowed for simplifying the implementation of inverse kinematic of the designed parallel manipulator in the Matlab/Simulink environment. We have obtained virtual laboratory stand thanks to the connection of two computer design and simulation environments. There is the possibility of control system design and visualization of static and dynamic states of the three-dimensional model of a real object. The drawback of such approach is the necessity of taking into account accurate parameters of the real object. It requires detailed specification of numeric model designed in SimMechanics toolbox running in Matlab/Simulink environment.

As it comes from our analyses the initial virtual model is usually an approximation and it could be supplemented with details after the identification of the real object parameters. Besides, in case of computer simulation there appear some problems arising from numerical method used in the model, which may lead to the lack of convergence of numerical computation, for example in case of improper treatment of the mechanical system constraints.

The overall structure model of linear actuator drive with PM BLDS motor

The overall structure model of linear actuator drive is presented in Figure 6. PM BLDC motor model is the primary block of the shown structure. We have integrated in single block the components of motor model and electronic commutator model. Other blocks are responsible for matching the input circuit parameters and transforming rotary motion into linear.
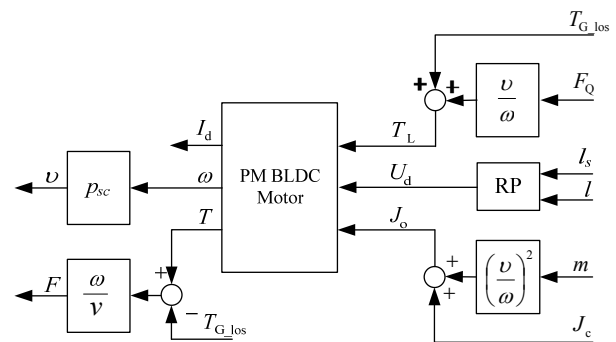

Fig.6. The block diagram of the linear actuator model drive with PM BLDC motor

Output quantities of the motor are DC power circuit voltage U_d, load torque T_L and moment of inertia of load converted to the motor output shaft J_L. Input quantities are DC circuit current I_d, angular velocity ω and motor torque T. The motor model is connected to the actuator model with a set of matching blocks, which convert quantities characteristic for linear screw drive to quantities specific for PM BLDC motor. The value of input voltage U_d is calculated by position controller (PC). The set point of the mentioned controller is translation of linear actuator l_s, which is determined by master control system. The matching blocks at the motor model inputs are responsible for load mass m and force F_L conversion to a signal proportional to the additional moment of inertia J_L and load torque T_L. However, the task of analogous matching blocks at the motor outputs is to convert signals proportional to angular velocity ω and motor torque T into signals referring to translational velocity of linear actuator v and force F, to which the movable part of that element is exposed. These matching blocks are based on then following relationships:
- block module of converting mass into moment of inertia:

(1)
$$J_o = m\left(\frac{v}{\omega}\right)^2 + J_c$$

- block module of processing load force into load torque:

(2)
$$T_L = \frac{v}{\omega} F_Q + T_{G\_los}$$

- block module of converting motor torque to linear actuator force:

(3)
$$F = \frac{\omega}{v} T - T_{G\_los}$$

where: J_c – moment of inertia of the drive clutch, J_o – additional moment of inertia converted to the motor output shaft; T_L motor load torque; T_{G_los} gear losses torque; F – force generated by the actuator, F_Q – force loading the linear actuator; m - part of the parallel manipulator load mass attributable to single actuator.

Modified model of PM BLDC motor

Due to extending simulation times of complete six-motor drive for parallel manipulator, we have decided to simplify one of the main components of the model. The accurate permanent magnet brushless DC motor model, which is available in Matlab/Simulink environment was the reference for the new model, which we have created for the purpose of the project described in the paper. The proposed model made possible simulation of static and dynamic states of PM BLDC motor. The diagram of three-phase brushless DC motor main circuit connections is presented in Figure 7. There is one pair of poles in the shown motor and the windings are connected in star. The electronic commutator structure is a three-phase bridge. A motor applied in the design of linear actuator is consistent with the schematic, except for four pairs of poles instead of one.
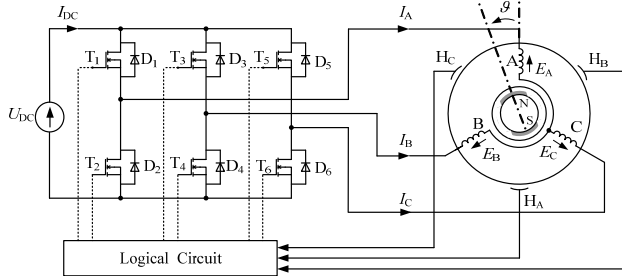

Fig.7. Wiring diagram for 3-phase PM BLDC motor with electronic commutator

The principle of operation and basic properties of PM BLDC motor are widely described in literature, for example in [11, 12, 22]. The most important relationships describing the motor are listed below:

(4)
$$e_k = \omega K_{fk}$$

(5)
$$T_{ek} = K_{fk} i_k$$

(6)
$$T_e = \sum_{k=A}^{C} T_{ek}$$

(7)
$$T = T_L + T_{los}$$

(8)
$$T_{dy} = J\frac{d\omega}{dt} = T_e - T$$

The following designations have been used: e_k - phase electromotive force (EMF); K_{fk} - excitation coefficient for k-th phase; T_{ek} – electromagnetic torque generated by k-th phase current, T_e – total electromagnetic torque of the motor; T, T_L and T_{los} – anti-torque, load torque and motor loss torque; T_{dy} – dynamic torque; J – total moment of inertia; ω – angular speed.

The motor with structure shown in Figure 6 can be brought [12, 11] into constant current equivalent model with structure illustrated by Figure 8. The main assumption of that operation is neglecting the difference between waveforms of back EMF, which is variable in PM BLDC motor and constant in case of typical DC motor. The other simplifying assumptions involve omission of the resistances and inductances of electronic commutator and motor terminals.
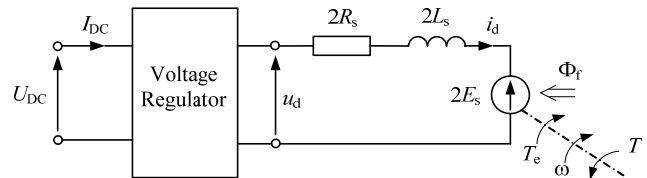

Fig.8. PM BLDC motor as a special case of a DC motor

For circuits with DC voltage controller or pulse-width modulation (PWM), the following relationships are true:

(9)
$$U_d = U_{d*} U_{DC}$$

(10)
$$I_d = \frac{1}{U_{d*}} I_{DC}$$

where U_{d*} is relative voltage value and U_{DC} is source dc voltage.

In case of ideal motor with negligible inductance impact, the following relationships are true:

(11)
$$\omega = \frac{U_d - 2R_s I_d}{2K_{fp}}$$

(12)
$$T_e = 2K_{fp} I_d$$

(13)
$$\omega_0 = \frac{U_d}{2K_{fp}}$$

(14)
$$\omega = \omega_0 - R_s \frac{I_d}{K_{fp}}$$

where K_{fp} is phase excitation coefficient for the flat section of phase EMF waveform.

In real motor, when the windings are switched, the currents do not instantly increase in a step-like manner, but they rise in accordance with exponential curve [12]. This causes emergence of additional voltage drops and increase in slope of torque-speed characteristic. What is more, due to energy recuperation into the source during the time when backward diodes conduct current, the current producing electromagnetic torque I_e is greater than average input current I_d calculated for DC circuit, that is:

(15)
$$I_e = \frac{T_e}{2K_{fp}} > I_d$$

The additional voltage drops may be taken into account by introducing the commutation impact coefficient, which provides information on how many times the voltage drop due to commutation is greater than voltage drop across the resistance. If we refer to [12], we find that commutation coefficient defined as:

(16) $$k_\mathrm{Q} = \frac{U_\mathrm{dx}}{U_\mathrm{R}}$$

will be defined as follows, when slight simplifying assumptions have been adopted:

(17) $$k_\mathrm{Q} = \frac{mp}{2\pi}\frac{\omega L_\mathrm{s}}{2R_\mathrm{s}}$$

The most important of all simplifying assumptions is that during commutation motor speed remains approximately constant. When commutation coefficient is used (16), (14) may be reduced to:

(18) $$\omega = \omega_0 - R_s\left(1 + k_\mathrm{Q}\right)\frac{I_\mathrm{e}}{K_\mathrm{fp}}$$

When commutation coefficient (17) is introduced into (18), we obtain:

(19) $$\omega = k_\mathrm{ch}\left(\omega_0 - R_\mathrm{s}\frac{T_\mathrm{e}}{K_\mathrm{fp}^2}\right) = k_\mathrm{ch}\omega_\mathrm{i}$$

wherein:

(20) $$k_{ch} = \frac{1}{1 + \dfrac{mp}{4\pi}\dfrac{L_s}{K_\mathrm{fp}}\dfrac{T_\mathrm{e}}{K_\mathrm{fp}}} = \frac{1}{1 + \dfrac{mp}{4\pi}\dfrac{L_s}{K_\mathrm{fp}}I_\mathrm{e}}$$

Coefficient k_ch represents additional slope of mechanical characteristic, where ω_i is angular speed of ideal motor with negligible inductance impact.

Basing on the relationships previously listed, which describe ideal PM BLDC motor, it is possible to develop a model with the structure identical to typical DC motor model structure. Such a model was denoted as modified model of PM BLDC motor [13]. The structure is shown in the Figure 9b.

Verification of numerical model of linear actuator

The numerical model of a single permanent magnet brushless DC motor propelled actuator was created on the basis of construction data of that element (Figure 10a). The model implemented in Matlab/Simulink environment has been used for development of parallel manipulator model as well as at the stage of PM BLDC motors selection for parallel manipulator design [7]. The model calculation has been accelerated in comparison with the typical PM BLDC motor numeric model, thanks to the implementation of previously described extension of DC motor model, based on the taking into account the slope of mechanical characteristic of the motor.

Another application of created model was the development and implementation of control algorithm. We have performed verification of a single actuator designed for the parallel manipulator on the laboratory stand shown in Figure 10b. The actuator was mounted in vertical position during tests. The PM BLDC motor was mounted in lower part of the actuator. Both simulation and laboratory tests, have been carried out for motor BG75x50PI, manufactured by Dunkermotoren company, with the following catalogue parameters: U_n= 24 V, p= 4, R_s= 20 mΩ, L_s= 0,125 mH, P_n= 431 W, T_n= 1,09 N.m J_M= 43,7$\cdot$10^{-6} kg.m2, T_los= 0,04 N.m, K_m= 52 mN.m/A, K_fp= 26 mV.s/rad.

Verification of the elaborated numeric model correctness was one of the aims of the laboratory tests of single actuator, designed for parallel manipulator. The evaluation of the model was based on the comparison of selected quantities, obtained by simulation research and during measurement of real object. The performed comparative

analysis also gave an opportunity to determine the effect of adopted simplifications. Besides, we have planned and partially conducted verification of requirements assumed at the design stage. We have performed the measurements using the test system presented in Figure 10b, equipped with CAN bus for acquisition of measured quantities.
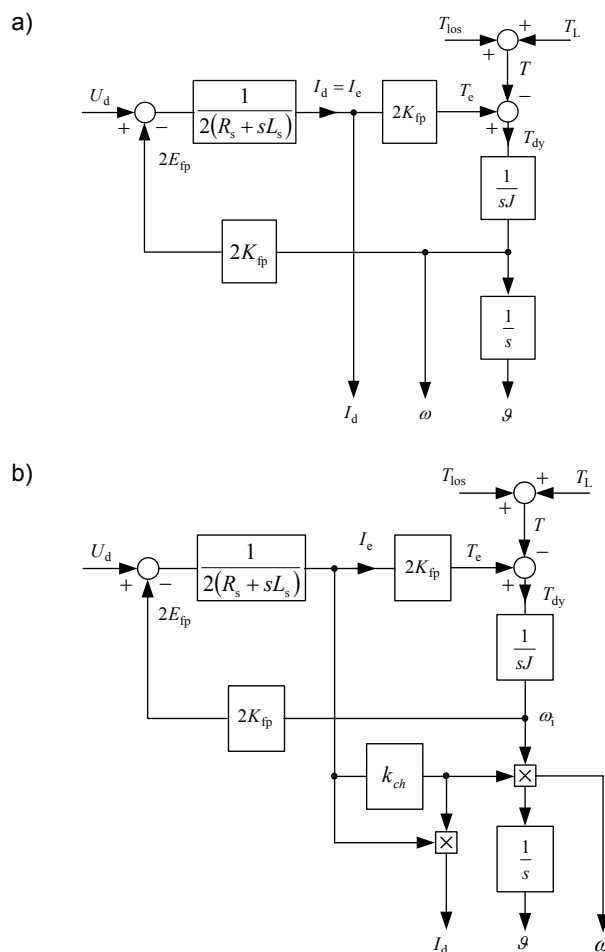

Fig.9. Models of PM BLDC motor: a) constant current model of PM BLDC motor; b) modified model of PM BLDC motor, which takes into account mechanical characteristics slope coefficient k_Ch

At first we have verified computer model of the PM BLDC motor. Figures 11 and 10 show the torque-speed characteristics of the motor obtained by measurements of real motor in comparison to the characteristics obtained from the simulation results. The tests have been run for voltages identical to those used during computer simulations. We have carried out the simulations using the modified constant current model, in which the influence of the inductance, as in real PM BLDC motor has been taken into account. As it comes from the diagram below, obtained simulation results are consistent with mechanical characteristics of real PM BLDC motor in range of nominal load torque. Figure 13 shows waveforms of translation l of the linear actuator, velocity n of the motor and current drawn from the voltage source I_{DC}. There are presented simulation results (Figure 13a) and measurements of the real motor (Figure 13b). We have obtained the waveforms for set stroke length l_s= 330 mm and for rotational velocity 800 rpm. The presented simulation results were acquired for control system structure, where master position controller was implemented.
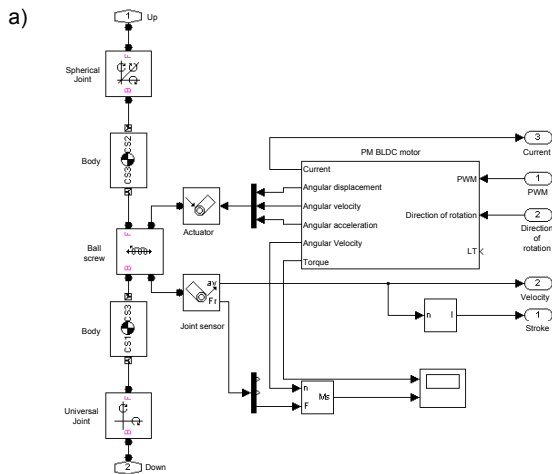
a)

Fig.12. Mechanical characteristics ω = f(T_e) obtained for the motor powered with voltage of 24V for PM BLDC model from Matlab/Simulink library and for modified DC model of that motor.

Summary and conclusions

On the basis of performed work in range of computer modelling and on the basis of the laboratory verification of permanent magnet brushless DC motor, loaded with the ball screw linear actuator, we could state that numeric model, worked out for the research, is correct and allows for calculating acceleration with assumed accuracy. Obtained simulation results are consistent with laboratory tests measurements, although some simplifications have been applied relative to accurate full PM BLDC motor model.

The developed model of PM BLDC motor with electronic commutator gives possibility to determine average rotational velocity and current values, with proper accuracy. The obtained results are similar to those, which are available in case of application of library model of PM BLDC motor from Matlab/Simulink simulation environment. However, in case of modified model application, the simulation times are significantly reduced. The model that we developed, is suitable for simulation of multi PM BLDC motor drives. In order to achieve correct simulation results, the switching period of commutator valves should be lower than electromechanical time constant of the motor.

In range of PM BLDC motor control we have applied the CAN bus as an interface, connecting master computer control system with the motor equipped with built-in power electronics converter and controller. Despite the lack of application of real time operating system in the computer controller, we have noted proper operation of the controlled drive system. On the basis of the process and results of the laboratory research, we could state, that developed control architecture is suitable for digital recording of measured quantities through internal motor controller. We have found, that in case of final control system for six PM BLDC motors drive implementation, it is advantageous to apply real time operation system. Another solution for that control system is based on the development of dedicated controller with DSP microcontroller or other motion class controller. Moreover, due to the planned further laboratory tests of multi motor drive for parallel manipulator, it is useful to carry out the verification of laboratory control system based on LabVIEW computing environment, seen as an alternative to the currently used computer control system based on the tools provided by the motor manufacturer.

b)

Fig.10. Linear actuator a) numerical model; b)view of the measuring system

Measured operational parameters of the motor were acquired by internal built-in sensors and transferred to the host computer using CAN bus. The test results were stored in a file on the computer controlling the motor also through CAN interface. During the measurements the linear actuator was not loaded with any additional mass.
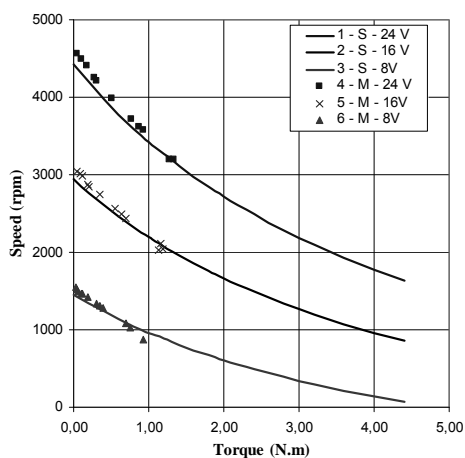

Fig. 11. Torque-speed characteristics of the modified constant current model motor obtained by computer simulations (1, 2, 3) for three supply voltage values (24V, 16V and 8V) and measurement results (4, 5, 6) obtained for identical voltages.
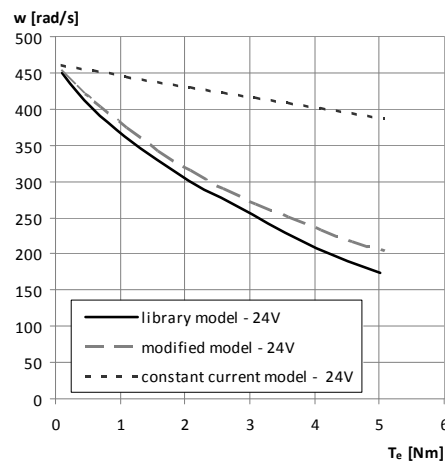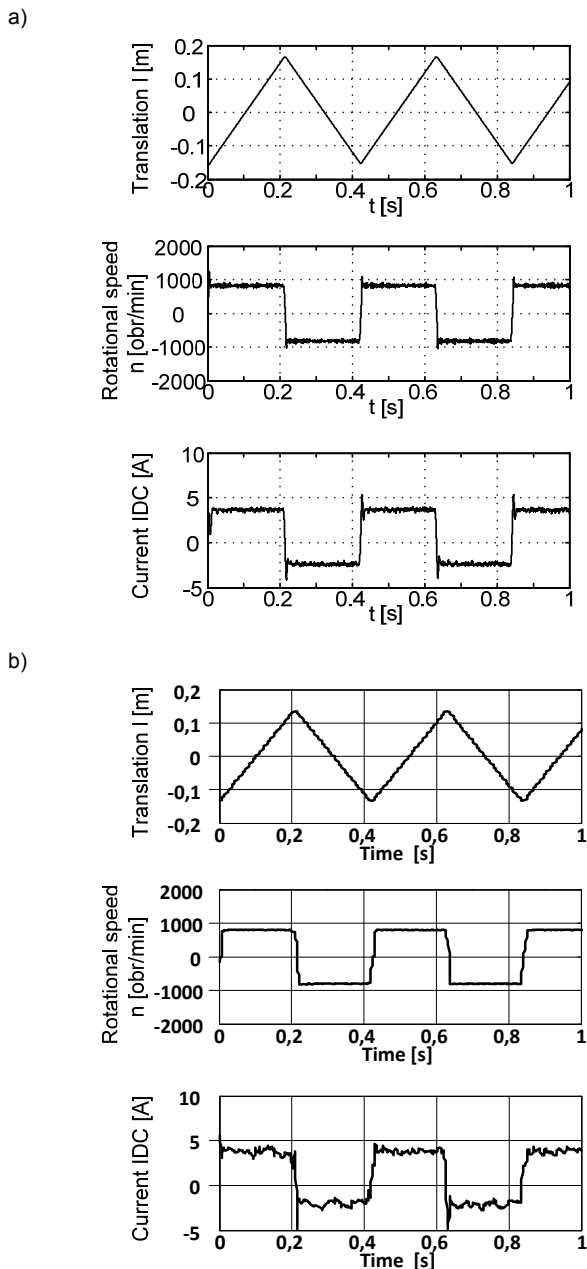
a)

b)

Fig.13. The recorded waveforms of translation *l*, rotational velocity *n* and current I_{DC} of actuator drive for: a) simulations; b) measurements

REFERENCES

[1] Bhandari, V. B., Design of Machine Elements, *Tata McGraw-Hill Education*, (2010).
[2] Blaise, J., Bonev, I., Monsarrat, B., Briot, S., Lambert, J., Perron C., Kinematic characterisation of hexapods for industry, *Industrial Robot: An International Journal*, (2010), Vol. 37, Issue 1, pp.79 – 88.
[3] Březina, L., Andrš, O., and Březina, T., NI LabView – Matlab SimMechanics Stewart platform design, *Applied and computational mechanics*, (2008), Vol. 2 (1), pp. 235-242.
[4] Brian, R., Hopkins, Robert, L., and Williams I., Kinematics, design and control of the 6-PSU platform, *Industrial Robot: An International Journal*, (2002), Vol. 29, Issue 5, pp. 443 – 451.
[5] Guojun, L., Zhiyong, Q., Junwei, H., and Xiaochu, L., Systematic optimal design procedures for the Gough-Stewart platform used as motion simulators, *Industrial Robot: An International Journal*, (2013), Vol. 40 Iss: 6, pp.550 – 558.
[6] Guojun, L., Zhiyong, Q., Xiaochu, L., and Junwei, H., Tracking performance improvements of an electrohydraulic Gough-Stewart platform using a fuzzy incremental controller, *Industrial Robot: An International Journal*, (2014), Vol. 41, Issue 2, pp.225 – 235
[7] Hetmańczyk, J., Gawleta, Ł., and Krykowski K., A computer model of a parallel multi-drive manipulator of brushless DC motors" (in Polish), *Electrical Machines - Transaction Journal*, (2013), No. 98/2013, pp. 159-162.
[8] Hüseyin, A., Elmas, A., Ibrahim Ö., Neural network algorithm for workspace analysis of a parallel mechanism, *Aircraft Engineering and Aerospace Technology*, (2007), Vol. 79, Issue 1, pp.35 – 44.
[9] Jianwei Ch., Xiaoxian Y., Control of Electric Actuator Using Brushless DC Motors and Its Performance Evaluation, *IEEE Second International Conference on Intelligent Computation Technology and Automation*, (2009). ICICTA '09, pp. 38 – 41.
[10] Kania, L., Dziurski, A., and Kasprzycki, A. (2012), "The Examples of the calculation of the basics of machine design" (in Polish), WNT Warszawa.
[11] Krishnan, R., Electric Motor Drives, Modelling, Analysis and Control", *Prentice Hall*, *New Jersey*, (2001) .
[12] Krykowski, K., PM BLDC motor in electric drive. Analysis, properties, modelling" (in Polish), *Silesian University of Technology*, (2011) Gliwice.
[13] Krykowski, K., and Hetmańczyk, J., Constant Current Models of Permanent Magnet Brushless Direct Current Motor, *Topical Problems in the Field of Electrical and Power Engineering - Pärnu* (2013), Talin – Pärnu Estonia, pp. 175 – 179.
[14] Krykowski, K., Hetmańczyk, J., and Makieła D., Impact of windings switching on torque-speed curves of PM BLDC motor, *COMPEL - The International Journal for Computation and Mathematics in Electrical and Electronic Engineering*, (2013), Vol. 32, Issue 4, pp. 1300 – 1314.
[15] Lopes, A.M. and Almeida, F. G., Acceleration-based force-impedance control of a six-dof parallel manipulator, *Industrial Robot: An International Journal*, (2007), Vol. 34, Issue 5, pp.386 – 399.
[16] Merlet, J.P., Parallel Robots, *Springer Science & Business Media*, (2006).
[17] Mutlu, H., Akçali, İ., D., and Gülşen, M., A Mathematical Model for the Use of a Gough-Stewart Platform Mechanism as a Fixator, *Journal of Engineering Mathematics*, (2006), Vol. 54, Issue 2, February, pp. 119 – 143.
[18] Qiang Meng, Tao Zhang, Jingfeng He, Jingyan Song, and Xuedong Chen, Improved model-based control of a six-degree-of-freedom Stewart platform driven by permanent magnet synchronous motors, *Industrial Robot: An International Journal*, (2012), Vol. 39, Issue 1, pp. 47 – 56.
[19] Sajkowski, M., and Krykowski, K., Control system design using rapid prototyping methods on an examples of voice controlled mobile robot and 6DOF parallel manipulator, *XXIII Symposium Electromagnetic Phenomena in Nonlinear Circuits - EPNC*, (2014) , Pilsen, Czech Republic, pp. 155-156.
[20] Sewoong K., Modeling and fault analysis of BLDC motor based servo actuators for manipulators, *IEEE International Conference on Robotics and Automation, ICRA,* (2008), 19-23 May, pp.767 - 772.
[21] Stenzel, T., Sajkowski, M., and Grzesik, B., Design and Implementation of 6-DOF Parallel Manipulator Driven by Permanent Magnet Brushless DC Motors, *18th International Conference on Methods and Models in Automation and Robotics, MMAR*, (2013), pp. 372 - 377.
[22] Zawirski K., Control of synchronous motor with permanent magnets" (in Polish), *Poznań University of Technology*, *Poznań,* (2005).

Authors: dr inż. Janusz Hetmańczyk, dr inż. Tomasz Stenzel, dr hab. inż. Bogusław Grzesik prof. Pol. Śl., Silesian University of Technology, Faculty of Electrical Engineering, Department of Power Electronics, Electrical Drives and Robotics, Bolesława Krzywoustego 2, 44-100 Gliwice, Poland, E-mail: Boguslaw.Grzesik@polsl.pl; Janusz.Hetmanczyk@polsl.pl; Tomasz.Stenzel@polsl.pl .